The dissipation in Landauer's ballistic resistor

Eric Bringuier

The dissipation in Landauer's ballistic resistor

Eric Bringuier

Matériaux et Phénomènes Quantiques
Unité mixte 7162 CNRS & Université de Paris 7, case 7021
5 rue Thomas Mann, 75205 Paris Cedex 13, France

The Joule heating effect inherently associated with an electrical resistance involves dissipation and irreversibility, which are not contained in the present-day wave-mechanical account of the Landauer ballistic conductance. This work makes use of non-equilibrium thermodynamics, where dissipation is quantitatively defined as the rate of entropy production, to describe the transports of electric charge and entropy and to map the dissipation in a ballistic resistor. Using the Vlasov kinetic equation with suitable boundary conditions, it is demonstrated that intensive thermodynamic variables are well-defined inside a ballistic resistor subjected to a weak applied voltage. It is shown that dissipation occurs only in the terminals. The prediction of a uniform electrochemical potential is supported by a four-point probe measurement of resistance in a constriction of the electron gas present at a GaAs/AlGaAs heterojunction. The work also predicts a flat temperature profile inside a ballistic resistor whose terminals have distinct temperatures. The map of isothermal entropy production is studied analytically in the simplest ballistic device, namely a planar vacuum diode. The study shows the vastly discrepant behaviours of the electrochemical and electric potentials and the necessity of a non-equilibrium treatment of screening. Implications are drawn for solid-state ballistic resistors.

Keywords: Landauer conductance; dissipation; non-equilibrium thermodynamics; ballistic transport; vacuum diode

1. Statement of the issue

In 1981 Landauer asked the question "Can a length of perfect conductor have a resistance?", where "perfect" meant that over the given length the conduction electrons travel ballistically, i.e. without undergoing a collision with the lattice of atoms [1]. Landauer's calculation of the electric current I in response to a small voltage U applied between the two terminals to a metallic perfect wire threw up a linear relationship $I = GU$ where the electrical conductance G was found to be $\overline{t}(2e^2/h)$, with e denoting the elementary charge and h Planck's constant. An average wave-mechanical transmission coefficient $\overline{t}$ of electrons between the two terminals should be included because a motion allowed in classical mechanics has a probability less than unity in quantum mechanics. Shortly thereafter, Sinkonnen *et al.* [2] investigated the same question for a semiconducting wire where the electron statistics is non-degenerate, i.e. the occupancy of electron states is much less than unity. Then, the formula for G contains an extra occupancy factor. Moreover, the calculated conductance decreases as L^{-1} at lengths L longer than the electronic mean free path because of collisions occurring in the wire; and for L of a few atomic layers, an increase of G is expected as $\overline{t}$ is enhanced by tunnelling through classically forbidden states.

The first experiments answering Landauer's question were performed in 1988 on degenerate GaAs wires at a low temperature, where the electronic mean free path can reach several micrometres [3, 4]. The wires were electrostatic constrictions of the quasi-two-dimensional electron gas lying on the GaAs side of a GaAs/GaAlAs heterojunction. The observed conductance was finite and exhibited quantization in approximate multiples of $2e^2/h$. The latter feature and other ones had not been anticipated by theory, as was remarked by van Houten *et al.* [5] and by Landauer [6]. The quantization

of conductance was later observed on metal wires [7, 8]. It could be related to the fact that a constriction of the electron flow acts as an electron wave guide with a finite number of discrete transverse eigenmodes, now termed conduction channels. Each one has a conductance approximately equal to $2e^2/h$. In the present paper, we shall have in mind the "perfect conduction" observed in such constrictions of a GaAs electron gas. While in Cu the electron density is about 10^{29} m^{-3}, in a quasi-one-dimensional constriction of the GaAs electron gas it is about 10^{24} m^{-3}. The high conductivity of the GaAs wire is made possible by the very high electrical mobility ($\geq 10^2$ m^{2}V^{-1}s^{-1}) stemming from the virtual lack of static disorder, the separation of conduction electrons (in GaAs) from ionized donors (in AlGaAs) and the low temperature freezing the lattice vibrations so that only the spontaneous emission of phonons is possible.

Ohm's linear law $I = GU$ is accompanied with a Joule heating effect because the generator which maintains a steady voltage across a resistor delivers a steady electric power $UI = GU^2$ manifested as heat. The release of heat is an irreversible and dissipative process. As Landauer [9] had remarked in 1987, "if energy is to be dissipated, e.g. through a conductance, where does it go? Physicists have developed remarkable cleverness in starting from conservative Hamiltonian dynamics, which is easiest to treat, and using it to predict dissipative behavior, which is prevalent. Much of this, however, is based on cheating. A Hamiltonian system with a limited number of degrees of freedom is, of course, just that. It can store energy, it cannot dissipate it." Because $G \propto \overline{t}$, the theoretical picture of ballistic conduction in GaAs wires reached in 1999 is summed up in the statement "Conductance is transmission" [10, 11]. But Imry and Landauer [11] remind us that "the dissipation and the irreversibility are in the reservoirs; carriers returning to them from the sample eventually suffer inelastic collisions". Again the authors remark that dissipation cannot arise in a purely quantum-mechanical account of ballistic conduction: "Quantum theory, as described by the Schrödinger equation, is a theory of conservative systems, and does not allow for dissipation. [...] Some supplementary handwaving is needed to calculate a dissipative effect such as conductance, for a sample with boundaries where electrons enter and leave".

In view of those remarks the purpose of the present paper is to examine the conduction observed in ballistic resistors from the standpoint of non-equilibrium, or irreversible, thermodynamics, where dissipation is quantitatively defined as the rate of entropy production [12, 13]. We shall use that thermodynamics to address the question "Where is the resistance?" asked by Datta [14]. He answered that the measured resistance G^{-1} consists of an internal resistance, which vanishes and increases together with the wave-mechanical reflection coefficient $1 - \overline{t}$, in series with contact resistances associated with the terminals. The latter are electron reservoirs to which the ballistic region is connected. In that view, dissipation would occur in the contact resistances while the internal resistance, associated with reflection, would be non-dissipative. That view is subsequently held by other authors [15-18]. But it is deemed unsatisfactory by Das and Green [19, 20]; and it is not entirely shared by Lesovik and Sadovskyy [18] who state that "the Joule heat dissipates far from the reservoirs due to slow energy relaxation" (they do not assess the rate of energy relaxation, however). In Gurevich's theory [21], the Joule heating occurs in the reservoirs; but that theory assumes reflectionless transport through the structure, i.e. $\overline{t} = 1$, so that no resistance due to reflection can arise.

We will use the tools of thermodynamics in another perfect conductor in Landauer's sense, namely a portion of vacuum between two parallel metallic plates. A metal-vacuum-metal device is a vacuum diode, or valve. It is akin to Landauer's perfect conductor since electron transport in vacuum is ballistic and the current at saturation is proportional to a wave-mechanical transmission coefficient [22, 23]. Electrons in a vacuum obey Maxwell's non-degenerate statistics, and indeed the possibility of a non-degenerate perfect conductor had been anticipated shortly after Landauer's question [2]. A valve exhibits a non-linear current-voltage relationship $I \propto U^{3/2}$ at a high U [24, 25]; but we have calculated a linear relationship $I \propto U$ at a low U [26]. The low-voltage dI/dU is given by a Landauer formula where the non-degenerate nature of the statistics entails an extra occupancy factor in G; see appendix A. In short, a vacuum diode has very many conduction channels which are weakly occupied. The calculated dI/dU agrees with the manufacturer's data sheet [26]. A vacuum diode is operated at a high temperature to ensure a significant thermionic emission of electrons to vacuum. In contrast, a solid-

state wire must be cooled to a very low temperature to ensure an electronic mean free path exceeding the wire length [3-5]. The mean free path is maximized at a vanishing temperature such that electron-lattice scattering reduces to spontaneous phonon emission only. In vacuum, no cooling is necessary because no lattice prevents the electrons from travelling ballistically, whatever the temperature. Compared to a metallic or semiconducting wire, the key advantages of the vacuum diode are its simpler physics and geometry. In this paper, the same thermodynamic framework will be used to shed light on dissipation in a vacuum diode and in a solid wire.

The paper is organized as follows. Section 2 first recalls the non-equilibrium-thermodynamic framework describing the transports of electric charge and heat in an ordinary conductor and the attendant dissipation. Then, to check the legitimacy of that framework in a terminal–ballistic-conductor–terminal structure, we make use of kinetic theory which gives the spatial behaviour of the steady-state occupation function. This provides the spatial behaviour of the dissipation in Section 3. In the isothermal case, the predicted dissipation is checked against a four-point probe measurement of resistance in a GaAs ballistic wire. The non-equilibrium-thermodynamic result is contrasted with previous quantum-mechanical considerations ignoring entropy production. Section 4 works out an analytical model of the Joule heating effect in a vacuum diode, and draws implications for solid-state ballistic conductors. The paper is concluded in Section 5.

2. Dissipation and the Joule heating effect in non-equilibrium thermodynamics

2.1. *The framework of non-equilibrium thermodynamics*

To properly address heating and dissipation in an electric resistor, one should explicitly consider the flow of heat and the possibility of an inhomogeneous temperature T. No magnetic field will be considered in this paper. The simplest framework is the one of non-equilibrium thermodynamics [12]. Its relationship with the Boltzmann kinetic theory is well understood [13]: they agree with one another when thermodynamic equilibrium is weakly perturbed. Equilibrium in a resistor is obtained under no voltage and no temperature difference between the terminals. Non-equilibrium thermodynamics is a valid framework under *weak voltage* and *weak temperature difference* entailing weak current densities. In a medium of constant volume, the appropriate thermodynamic function is the Helmholtz free energy. Let $a(n, T)$ denote its value per particle (conduction electron), where n is the particle density. The function a provides the entropy per particle $s = -(\partial a/\partial T)_n$ and the chemical potential $[\partial(na)/\partial n]_T$. Adding up the electrical energy $\bar{e}V$, where $\bar{e} = -e$ is the signed electron charge and V is the electric potential, yields the electrochemical potential $\tilde{\mu}$. The voltage between two points is the difference of their electrochemical potentials per elementary charge. For example, while the voltage across the terminals of a *p-n* junction diode in equilibrium is zero, the electric-potential difference is about 1 V in a silicon diode [27, 28]. In non-equilibrium thermodynamics $\tilde{\mu}$ and T are defined locally and their gradients give rise to an electron-current density $\mathbf{j}$ and a heat-current density $T\mathbf{j}_S$ where $\mathbf{j}_S$ is the entropy-current density [12, 13]. The dissipation $\dot{\Sigma}$ is the local production of entropy per unit time and unit volume,

$$\dot{\Sigma} = \frac{1}{T}\left[\mathbf{j}\cdot\boldsymbol{\nabla}(-\tilde{\mu}) + \mathbf{j}_S\cdot\boldsymbol{\nabla}(-T)\right]. \tag{1}$$

The current densities are related to the gradients through linear relations which may be written in several equivalent ways. The one most convenient to our purpose is

$$\mathbf{j} = n\mu\left[\boldsymbol{\nabla}(-\tilde{\mu}) - (s + s^*)\boldsymbol{\nabla}T\right], \tag{2}$$

$$\mathbf{j}_S = -\kappa\left(\frac{\boldsymbol{\nabla}T}{T}\right) + (s + s^*)\mathbf{j}, \tag{3}$$

where μ is the electron mechanical mobility (drift velocity per unit applied force, or inverse friction coefficient), κ is Fourier's thermal conductivity and s^* is the entropy of transport, following the nomenclature and notation of [29]. While s is an equilibrium-thermodynamic function, the extra term s^* is not; its kinetic nature can be seen in microscopic models where s^* is related to relaxation rates [12]. While s depends on how entropies are gauged, s^* does not [30]. In the linear-response relations (2)-(3), the first term on the right-hand side expresses the fact that electrons (entropy) flow(s) down

the electrochemical (temperature) gradient, and the second term is the Seebeck (Peltier) contribution to $\mathbf{j}$ ($\mathbf{j}_S$).

If T is homogeneous, $\mathbf{j}$ reduces to $n\mu\nabla(-\tilde{\mu})$. If also n is homogeneous, $\nabla(-\tilde{\mu})$ reduces to the electric force $\nabla(-\bar{e}V)$ so that relation (2) is just Ohm's local law $\bar{e}\mathbf{j} = e^2 n\mu\nabla(-V)$ with electrical conductivity $e^2 n\mu$. If T is not homogeneous, relation (2) includes the Seebeck thermoelectric effect: the flow of carriers between two points is due not only to the voltage, but also to the temperature difference, between the points. By breaking up $\tilde{\mu} = h - Ts$ into energetic (h) and entropic ($-Ts$) contributions, relation (2) is rewritten as

$$\mathbf{j} = n\mu(-\nabla h + T\nabla s - s^*\nabla T). \tag{4}$$

The force $-\nabla h + T\nabla s - s^*\nabla T$ driving carriers is the sum of three contributions: the first one is directed towards lower energies h, the second one towards higher entropies s, and the third one is unrelated to an equilibrium-thermodynamic function.

The dissipation $\dot{\Sigma}$ is rewritten by bringing relations (2) and (3) into (1), whence

$$\dot{\Sigma} = \frac{1}{\mu}\left(\frac{\mathbf{j}^2}{nT}\right) + \kappa\left(\frac{\nabla T}{T}\right)^2. \tag{5}$$

The positivity of $\dot{\Sigma}$ is due to the positivity of the friction coefficient $1/\mu$ and of thermal conductivity κ. The first contribution to $\dot{\Sigma}$ is a generalized Joule-heating term where the overall driving force $-\nabla h + T\nabla s - s^*\nabla T = \mathbf{j}/n\mu$ replaces the electrical force $\nabla(-\bar{e}V)$. Irreversibility, i.e. $\dot{\Sigma} > 0$, is caused firstly by the friction undergone by the carriers dragged off by the driving force and secondly by Fourier's flow of heat from hot to cold locations. Dissipation due to a flow of heat can cause damping in the same way as friction [31].

2.2. *The validity of the framework in a ballistic conductor*

The above framework holds if the particles have well-defined values of their intensive thermodynamic variables at every location. This condition is met in ordinary conductors, where the scattering rate of conduction electrons is high. Taking Cu at 1 K as an example, the electrical conductivity $e^2\mu n \approx 5\text{x}10^{10}\ \Omega^{-1}\text{m}^{-1}$ and the electron density $n \approx 10^{29}\ \text{m}^{-3}$ yield $\mu \approx 2\text{x}10^{19}$ s/kg. From the Drude formula, the scattering rate $1/\tau$ is estimated to be $5\text{x}10^{10}\ \text{s}^{-1}$. Therefore electrons can quickly reach a state of equilibrium characterized by a Fermi-Dirac occupancy of the states, with well-defined variables $\tilde{\mu}$ and T. The latter is also the temperature of the lattice because an electron exchanges energy with it at a rate close to $1/\tau$. In a steady state where current densities $\mathbf{j}$ and $\mathbf{j}_S$ are flowing, the deviation from equilibrium decreases with decreasing current densities. To the first order in $\mathbf{j}$ and $\mathbf{j}_S$, the steady-state occupancy of the electron states,

$$f(\mathbf{p},\mathbf{r}) = f_0(E_k(\mathbf{p}),\mathbf{r}) + f_1(\mathbf{p},\mathbf{r}), \tag{6}$$

is the sum of an isotropic function f_0 and of a small dipolar contribution f_1 odd in $\mathbf{p}$ so that $\mathbf{j}$ and $\mathbf{j}_S$ are small but do not vanish. In (6), $E_k(\mathbf{p}) = \mathbf{p}^2/2m^*$ for electrons of effective mass m^*; and, in case of confinement along y and z in a transverse eigenmode of a wire, $E_k = p_x^2/2m^* + E_\perp$ with $E_\perp$ taking discrete values. The isotropic contribution f_0 is a Fermi-Dirac function of the total (mechanical) energy $E = E_k(\mathbf{p}) + \bar{e}V(\mathbf{r})$ with local, position-dependent $\tilde{\mu}(\mathbf{r})$ and $T(\mathbf{r})$. This is the so-called state of local equilibrium where the deviation from equilibrium f_1 is much smaller than f_0 [13, 32, 33].

Granted local equilibrium in the electrodes, or terminals, made up of ordinary conductors lying at $x < 0$ and $x > L$, we ask the question whether conduction electrons have well-defined values of $\tilde{\mu}$ and T in a ballistic conductor lying in the range $0 < x < L$. This amounts to asking whether $f(\mathbf{p},\mathbf{r})$ has a Fermi-Dirac shape. The answer can be obtained from kinetic theory [32, 34] where the occupancy $f(\mathbf{p},\mathbf{r},t)$ at time t obeys a Vlasov equation,

$$\frac{\partial f}{\partial t} + \mathbf{v}_g(\mathbf{p})\cdot\nabla f + \nabla(-\bar{e}V)\cdot\left(\frac{\partial f}{\partial \mathbf{p}}\right) = 0, \tag{7}$$

$\mathbf{v}_g(\mathbf{p}) = \partial E_k/\partial\mathbf{p}$ is the group velocity, and the electrical force $\nabla(-\bar{e}V)$ undergone by a carrier is determined self-consistently from the Poisson equation. In one dimension, the latter is

$$\frac{\mathrm{d}^2V}{\mathrm{d}x^2} + \frac{\bar{e}n(x)}{\varepsilon} = 0, \tag{8}$$

where ε is the permittivity of the conductor. The Vlasov equation is just a collisionless Boltzmann kinetic equation where the right-hand side vanishes owing to a vanishing collision rate. In the gap of a vacuum diode, $1/\tau$ vanishes because there is no lattice; the electron only undergoes the electrical force $\nabla(-\bar{e}V)$. On the GaAs side of a GaAs/AlGaAs heterojunction, $1/\tau$ is very low because the mobility $\mu \approx \tau/m^*$ is very high.

A steady-state, isotropic solution $f_0(E_k(\mathbf{p}), \mathbf{r})$ of Eq. (7) satisfies:

$$\mathbf{v}_g(\mathbf{p})\cdot\left[\nabla f_0 + \left(\frac{\partial f_0}{\partial E_k}\right)\nabla(-\bar{e}V)\right] = 0, \tag{9}$$

at any $\mathbf{p}$ and $\mathbf{r}$, so that the term in square brackets vanishes. Letting $f_0(E_k, \mathbf{r}) = F(E, \mathbf{r})$, the term in square brackets is ∇F. The vanishing of ∇F means that $F = F(E)$ and reflects the conservation of the mechanical energy E of a conduction electron in ballistic transport. The function F should fulfil continuity conditions at the boundaries $x = 0$ and L. Granted local equilibrium in the electrode lying at $x < 0$, F at the boundary $x = 0$ has to be a Fermi-Dirac function with the parameters $\tilde{\mu}$ and T of the electrode at $x = 0$:

$$F(E) = \left[\exp\left(\frac{E - \tilde{\mu}(0)}{kT(0)}\right) + 1\right]^{-1}. \tag{10}$$

Therefore, in the ballistic region f_0 is a Fermi-Dirac function of E with position-independent parameters $\tilde{\mu}_v = \tilde{\mu}(0)$ and $T_v = T(0)$. By the same token, because of local equilibrium in the electrode lying at $x > L$, we also have $\tilde{\mu}_v = \tilde{\mu}(L)$ and $T_v = T(L)$. The ballistic region thus acts as a short-circuit equalizing the electrochemical potentials at its ends, and where the temperature profile is flat.

Three points are worth noting here. First, the right-hand side of Eq. (9) is taken as zero while actually it is of the order of f_0/τ. It may be neglected if it is much lower than either term on the left-hand side, e.g. $\mathbf{v}_g(\mathbf{p})\cdot\nabla f_0 \approx v_g f_0/L$. As $v_g\tau$ is the electronic mean free path, this is just the condition $L << v_g\tau$ expressing the ballistic nature of transport over length L. Secondly, the flat electrochemical potential profile in the ballistic region is reminiscent of the behaviour of the junction of a metal with a high-mobility semiconductor (Schottky diode). In the semiconductor, the profile of electrochemical potential is flat under direct bias or weak reverse bias; the junction is then governed by the ballistic ("thermionic"), instead of diffusion, theory [35]. The profile of electrochemical potential behaves in a similar way in the practical implementations of a ballistic resistor which are achieved in the high-mobility limit [3, 4]. Thirdly, the fact that transport is coherent in the ballistic region gives rise to transmission and reflection of an electron wave travelling forward (backward) from $x = 0^-$ (L^+) to $x = L^+$ (0^-), with wavevector $2\pi\mathbf{p}/h$ ($-2\pi\mathbf{p}/h$) in the range $0 < x < L$. The transmission and reflection coefficients take into account the multiple reflections and transmissions undergone by the wave at the boundaries, just like in a Fabry-Pérot interferometer in optics. The coefficients connect the anisotropic contributions f_1 on both sides of each boundary $x = 0$ or L so that current is conserved in the steady state, as happens in Ben Abdallah's model of quantum (coherent) transport in a layer connected to terminals where transport is semiclassical (incoherent) [36]. That model, just like ours, rests upon the Vlasov kinetic equation in the quantum (ballistic) region.

The next section addresses dissipation in the ballistic resistor and checks the non-equilibrium-thermodynamic picture of conduction against a four-point probe measurement of resistance in a solid-state resistor.

3. Non-dissipative transport in the perfect conductor

3.1. *The physics of entropy production*

The previous section has shown that the electron gas has well-defined intensive thermodynamic variables $\tilde{\mu}_v$ and T_v which are uniform in the ballistic region. Therefore we may now use the frame of thought of non-equilibrium thermodynamics of Section 2.1 with vanishing driving forces $\nabla\tilde{\mu}$ and ∇T. In relation (2) or (4), the overall driving force vanishes while the electron current density is finite. This is consistent since mobility $\mu \approx \tau/m^*$ is infinite in the ballistic region; we have to do with frictionless transport. The fact that a current density can flow under no driving force is akin to Newton's First Law in mechanics where a particle can have a finite velocity under no force. In the

ballistic region, transport is non-dissipative as the production of entropy $\dot{\Sigma}$ given by expression (1) vanishes although $\mathbf{j}$ and $\mathbf{j}_S$ do not. The vanishing of $\dot{\Sigma}$, which is due to $\nabla\tilde{\mu} = 0$ and $\nabla T = 0$, is in line with the conservation of *mechanical* energy [37] remarked above.

The absence of dissipation reflects the reversible nature of the transport phenomenon in the range $[0, L]$. For, if $f(\mathbf{p}, \mathbf{r}, t)$ satisfies the Vlasov equation, the time-reversed evolution $f(-\mathbf{p}, \mathbf{r}, -t)$ is also a solution of Eq. (7) with a velocity $\mathbf{v}_g(-\mathbf{p}) = -\mathbf{v}_g(\mathbf{p})$. In contradistinction, in the electrodes where transport can be described by a Boltzmann kinetic equation, the time-reversal invariance is broken by the scattering integral, which does not change sign upon $t \to -t$, on the right-hand side of that equation. This is the way irreversibility enters Boltzmann's H theorem [32, 34]. Reversibility is easier to grasp in the time-dependent regime described by kinetic theory than in the steady regime ($\partial f/\partial t = 0$) described by non-equilibrium thermodynamics. In the latter, irreversibility is assessed through the rate of entropy production $\dot{\Sigma}$, which vanishes in the ballistic region and takes positive values in the ordinary conductors making up the electrodes.

In Figure 1, the function $\tilde{\mu}(x)$ is shown to vary continuously from $x < 0$ to $x > L$. Function $T(x)$ varies in a similar way. Both functions exhibit gradients in the reservoirs ("c" lying at $x < 0$ and "a" lying at $x > L$) which serve as the contacting leads. It is in those non-ballistic conductors that dissipation $\dot{\Sigma}$ is non-zero. The Joule heating, which is the isothermal contribution to dissipation, occurs in the reservoirs where $1/\mu$ and $\nabla\tilde{\mu}$ are non-zero. Microscopically speaking, in an electron-lattice scattering event the exchanged energy is spread out at random over the huge number of degrees of freedom (vibrational modes) of the lattice, hence irreversibility and the production of entropy.

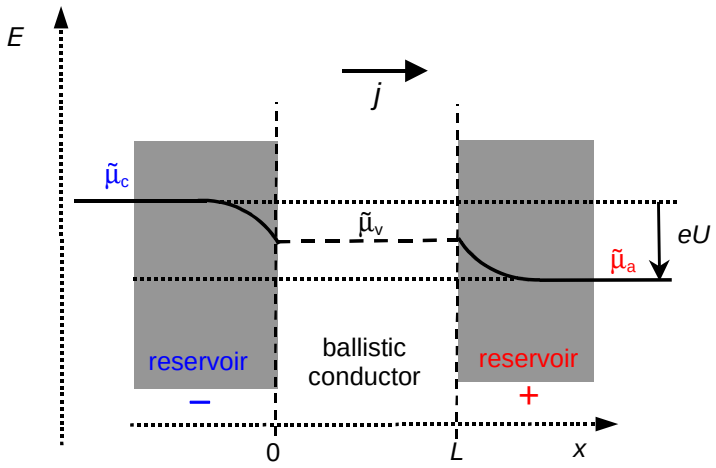

Figure 1. Energy diagram of the electrode–ballistic-conductor–electrode structure, showing the spatial variation of the electrochemical potential $\tilde{\mu}(x)$ of the electrons in the reservoirs (leads, or electrodes) and in the ballistic conductor, under a low bias $U = (\tilde{\mu}_c - \tilde{\mu}_a)/e$ causing electron current density j. (The bias has been exaggerated in the figure.) The slightly negative slopes $d\tilde{\mu}/dx$ far before $x = 0$ and far beyond $x = L$ have been approximated to zero on the figure because of the large electrical conductivity of reservoirs.

The temperature $T(x)$ of the conduction electrons might differ from that of the lattice vibrations in a solid ballistic conductor since electrons and phonons do not exchange energy. This is known in electron transport in sufficiently doped semiconductors: where the exchange of energy between electrons very much exceeds that with phonons, electrons have a temperature of their own that the electric field can raise well above that of the phonons [38]. But in the structure shown in Figure 1, the phonon and electron temperatures coincide outside the interval $[0, L]$ because of the strong electron-phonon scattering rates there. Since ballistic conduction inside the interval $[0, L]$ has been shown in Section 2.2 to entail the equality of the *electron* temperatures at $x = 0$ and L, the *lattice* temperatures at $x = 0$ and L will be equal as well. In other words, the perfect electrical conductor also

acts as a perfect thermal conductor or "thermal short-circuit". The vanishing of $T(0) - T(L)$ is compatible with a non-vanishing flow of heat because of the Peltier term in relation (3).

3.2. *Dissipation versus reflection as the origin of resistance*

The predictions of Section 2.2 are: (i) the electrochemical potential $\tilde{\mu}_v$ is uniform in the ballistic region of the resistor traversed by electron and heat currents; and (ii) the temperature T_v is uniform in that region traversed by currents. Prediction (i) implies that the ballistic region has a vanishing resistance defined as the ratio of the voltage drop to the electric current. Contrariwise, in the theoretical descriptions of [14-18], for one single conduction channel the resistance of the electrode–ballistic-conductor–electrode structure is written as a sum of three terms,

$$\frac{h}{2e^2\,\overline{t}} = \frac{h}{4e^2} + \left(\frac{1-\overline{t}}{\overline{t}}\right)\frac{h}{2e^2} + \frac{h}{4e^2}, \qquad (11)$$

and the non-zero central resistance on the right-hand side is ascribed to the finite wave-mechanical reflection coefficient $1 - \overline{t}$ of electrons traversing the structure.

A four-point probe measurement of resistance has been achieved on a 6-µm-long constriction making up a ballistic wire in GaAs near to an edge overgrown with AlGaAs [39]. When one single channel is obtained for a gate voltage lying between −4.5 and −3.8 V, figure 2 of [39] shows a quantized resistance ≈ 19 kΩ between the two current leads. That value is stronger than $h/2e^2 \approx 13$ kΩ because of "non-ideal coupling between the cleaved-edge-overgrowth wire and its two-dimensional source and drain contacts". Part of the electron wave is reflected as it leaves the source ("c") contact to enter the ballistic wire, and likewise at the drain ("a") contact. From Landauer's formula a non-ideal transmission $\overline{t} \approx 13/19 \approx 70$ % is inferred. From (11) one expects a central resistance 6 kΩ in series with a total contact resistance 13 kΩ. But the measured central resistance is zero since no voltage drop is observed between the two probes lying 2-µm apart in the 6-µm-long ballistic region. This is consistent with our prediction (i) that the electrochemical potential profile is flat within $[0, L]$. At this juncture, one may wonder to what extent the voltage probes are invasive since a voltmeter lowers the actual voltage present in a circuit if the voltmeter impedance does not largely exceed the resistance of the circuit under measurement. The impedance associated with each probe was found to be 250 kΩ so that the invasiveness is about 19/500 ≈ 4 % [39].

The internal voltage of the ballistic wire was measured to be half the source voltage reckoned with respect to the drain taken to be at ground; see figure 3 of [39] at a zero magnetic field. That is to say, $\tilde{\mu}$ in the wire is $(\tilde{\mu}_c + \tilde{\mu}_a)/2$. This is due to the symmetry of the device in the exchange of source and drain which changes I into $-I$.

In [14-18], the electrochemical potential is assigned well-defined values far before $x = 0$ and far after $x = L$, but not near $x = 0^-$ and $x = L^+$ where $\tilde{\mu}(0^-)$ and $\tilde{\mu}(L^+)$ are double-valued [14, 39]. Contrariwise, the present treatment follows non-equilibrium thermodynamics in considering that, in a reservoir of particles, $\tilde{\mu}$ is single-valued at any given location. When the reservoir delivers a small current of particles, there appears a small correction $f_1 \propto \nabla\tilde{\mu}$ to function f_0 with the latter keeping a local-equilibrium pattern characterized by a single-valued $\tilde{\mu}$ until $x = 0^-$ and $x = L^+$.

Regarding prediction (ii), to the author's knowledge no measurement of the temperature profile $T(x)$ has been reported in a GaAs ballistic wire with $T_c \neq T_a$; the profile in a vacuum diode is discussed in appendix A. For distinct T_c and T_a, the reasoning of [14, 39] entails a double-valued electron temperature near $x = 0^-$ and $x = L^+$. But this is impossible in a reservoir of energy which imposes a single-valued temperature at a given location, namely that of the phonons.

The following section illustrates how a finite electrochemical gradient arises from a finite mobility in a non-ballistic terminal, in contradistinction to the vanishing $1/\mu$ and $\nabla\tilde{\mu}$ in the ballistic region. Section 4.1 works out a specific model of dissipation in an isothermal planar vacuum diode, where the neglect of edge effects along y and z allows for analytical calculation of the electrochemical and electrostatic potentials, $\tilde{\mu}(x)$ and $V(x)$. An analytical calculation is not possible for the wire obtained by constricting the electron gas of a GaAs/AlGaAs heterojunction, where $\tilde{\mu}(\mathbf{r})$ and $V(\mathbf{r})$ are actually three-dimensional functions. Readers wishing to avoid the more technical aspects may proceed directly to Section 4.2.

4. Mapping the isothermal dissipation and the resistance

4.1. The Joule heating effect in a planar vacuum diode

From now on we only consider isothermal transport such that $T_c = T_v = T_a$. The functions $V(x)$ and $n(x)$ are governed by the Poisson and transport equation (2). Those equations should be supplemented by the dependence of the chemical potential $\tilde{\mu} - \bar{e}V = [\partial(na)/\partial n]_T$ on n in the cathodic ($x < 0$), non-dissipative ($0 < x < L$) and anodic ($x > L$) regions. In this subsection we illustrate the interplay of those equations on the example of a planar vacuum diode operated in the linear regime, i.e. under a low applied voltage. Since our purpose is one of fundamental physics, we shall consider here uncoated electrodes of a metal, e.g. tungsten, and calculate the profile of electrochemical potential whose gradient is proportional to the local Joule heating in a planar geometry. Specific values taken from Mullard's diode EB 91 (Siemens' EAA 91) will be used for definiteness [1].

Let $-x_c \approx 5\text{x}10^{-4}$ m denote the thickness of the cathodic plate. In the cathodic region $x_c < x < 0$, we break up $\tilde{\mu}(x)$ into two contributions,

$$\tilde{\mu}(x) = E_c(x) + E_F(x), \tag{12}$$

where $E_c(x) = E_c(x_c) + \bar{e}[V(x) - V(x_c)]$ is the bottom of the conduction band at location x, and $E_F(x)$, henceforth called the Fermi energy, is the filling height above the bottom. Let $n_+ = 6.3\text{x}10^{28}$ m^{-3} denote the atom density of tungsten. In a simple statistical-thermodynamic model of the metal, E_F is taken to depend on n as

$$E_F(n) = kT\ln\left[\frac{n}{N_c(T)}\right] \text{ if } n < n_d \text{ and } E_F(n) = E_{F0}\left(\frac{n}{n_+}\right) \text{ if } n > n_d, \tag{13}$$

where $E_{F0} \approx 12$ eV is the filling height in neutral tungsten [43], n_d is a cross-over density, $N_c(T) = g_s/\lambda_{dB}^3(T)$ is the effective density of states at the bottom of the conduction band [44], $g_s = 2$ is the spin multiplicity and $\lambda_{dB} = h/(2\pi m^* kT)^{1/2}$ is the thermal de Broglie wavelength. The second expression (13) holds for degenerate statistics, with an energy density of states n_+/E_{F0} independent of energy instead of varying as the square-root in the Sommerfeld (parabolic band) model [2]. Actually, at energies much in excess of kT above the conduction-band bottom, the density-of-states function is neither constant nor parabolic [43]. The first expression (13) holds for non-degenerate statistics, in the strongly depleted metal. Continuity of $E_F(n)$ at the cross-over density n_d and the fact that $E_{F0}N_c(T)/kTn_+ << 1$ yield

$$n_d \approx N_c(T)\left[1 + \left(\frac{E_{F0}}{kT}\right)\frac{N_c(T)}{n_+}\right] \text{ and } E_F(n_d) \approx E_{F0}\left[\frac{N_c(T)}{n_+}\right]. \tag{14}$$

Taking the effective mass m^* equal to the electron mass in vacuum m_0, it is computed that $n_d = 2.3\text{x}10^{26}$ m^{-3} and $E_F(n_d) = 0.033$ eV at $T = 1100$ K. As the first expression (13) becomes negative at $n < N_c(T) = 1.7\text{x}10^{26}$ m^{-3}, it cannot mean a conduction-band filling height. An electrochemical potential lying below the band bottom E_c means an effectively semiconducting medium.

The unknowns $V(x)$ and $n(x)$ at $x_c \le x < 0$ can be replaced by $E_c(x)$ and $n(x)$. We sketch the general scheme for obtaining them before solving a simple case. They obey the Poisson equation,

$$\frac{d^2E_c}{dx^2} = \frac{e^2}{\varepsilon}[n_+ - n(x)], \tag{15}$$

whenceforth ε is the permittivity of the metal, and the transport equation,

$$-\frac{dE_c}{dx} - \left(\frac{dE_F}{dn}\right)\frac{dn}{dx} = \frac{j}{n(x)\mu}, \tag{16}$$

---

[1] Actually, in a modern diode such as EB 91, the Joule heating is known to occur in the oxide-coated cathode [40]. This is understood from envisaging the diode as a series of resistors traversed by the same current: heating occurs in the most resistive layer, which is the oxide coating of the cathode; see [41, 42] in the high-voltage regime. The data sheet of EB 91 can be found on www.tubedata.info.

[2] Taking a parabolic-band relationship $E_F(n) = E_{F0}(n/n_+)^{2/3}$ changes equation (30) in appendix B into $d^2y/d\xi^2 - (5\eta/3)(1-y)^{-5/2}(dy/d\xi) + (2/3)[(1-y)^{3/2} - 1] = 0$. For $y << 1$, as occurs in the degenerate region, this is identical with equation (30) except for η becoming $5\eta/3$. Therefore the solution of the linearized equation (30) worked out in appendix B is not significantly affected by a parabolic choice for the $E_F(n)$ relationship.

where the force driving j is the sum of $-\mathrm{d}E_\mathrm{c}/\mathrm{d}x$, causing drift in the electric field, and $-\mathrm{d}E_\mathrm{F}/\mathrm{d}x$, causing diffusion from more to less populated places. In Eq. (16) mobility μ is taken to be independent of x because the variation of n prevails over that of μ in the electrical conductivity $e^2\mu n$. Three boundary conditions are needed at the entrance $x = x_\mathrm{c}$ of the cathodic plate. They are

$$E_\mathrm{c}(x_\mathrm{c}) = -E_\mathrm{F0}\,, \tag{17}$$

$$\left(\frac{\mathrm{d}E_\mathrm{c}}{\mathrm{d}x}\right)_{x=x_\mathrm{c}} = -\frac{j}{n_+\mu}\,, \tag{18}$$

$$n(x_\mathrm{c}) = n_+\,. \tag{19}$$

The first condition sets the reference level of energies; it is tantamount to letting $\tilde{\mu}(x_\mathrm{c})$, also denoted by $\tilde{\mu}_\mathrm{c}$, equal to zero. To set the reference level of electric potentials, we let $V(x_\mathrm{c}) = 0$. The second condition states that, far before the boundary $x = 0$ with the vacuum gap, the current density j is driven only by the electric force $F_\infty = j/n_+\mu$ with no contribution from diffusion. The third condition states that, far before the boundary $x = 0$, the metal is neutral; it is tantamount to $E_\mathrm{F}(x_\mathrm{c}) = E_\mathrm{F0}$.

The differential equations (15) and (16) and the boundary conditions (17)-(19) determine $E_\mathrm{c}(x)$ and $n(x)$ in the domain $x_\mathrm{c} \le x < 0$. Next, at the metal-vacuum boundary $x = 0$, the electric potential, electric displacement and electrochemical potential are continuous,

$$V(0^-) = V(0^+), \tag{20}$$

$$\varepsilon\left(\frac{\mathrm{d}V}{\mathrm{d}x}\right)_{x=0-} = \varepsilon_0\left(\frac{\mathrm{d}V}{\mathrm{d}x}\right)_{x=0^+}, \tag{21}$$

$$E_\mathrm{c}(0^-) + E_\mathrm{F}(n(0^-)) = \tilde{\mu}(0^+). \tag{22}$$

This provides three boundary conditions for the Poisson and transport equations in the vacuum gap at $x = 0^+$. The electron density $n(0^+)$ is given by $N_\mathrm{c}(T)\exp(-[\phi_0 + \tilde{\mu}_\mathrm{c} - \tilde{\mu}(0^+)]/kT)$ where ϕ_0 is the work function of the cathode [35]. The Poisson and transport equations subsequently determine $V(L^-)$, $(\mathrm{d}V/\mathrm{d}x)_{x=L-}$ and $\tilde{\mu}(L^-)$ just before the vacuum-metal boundary $x = L$. The continuity of electric displacement and of $\tilde{\mu}$ at $x = L$ provides $\mathrm{d}E_\mathrm{c}/\mathrm{d}x$ and $\tilde{\mu}$ just after the boundary. At the exit $x = x_\mathrm{a}$ of the anodic domain, n is given by a neutrality condition similar to (19) but involving the atom density in the anode. The anodic relationship $E_\mathrm{F}(n)$ differs from the cathodic one (13) if the two materials are different.

In what follows the coupled differential equations (15) and (16) are solved in the simple case of identical cathode and anode. Then, $\tilde{\mu}_\mathrm{v}$ lies half-way between $\tilde{\mu}_\mathrm{c}$ and $\tilde{\mu}_\mathrm{a} = \tilde{\mu}_\mathrm{c} - eU$ so that voltage U is equally shared between the cathodic and anodic plates. From relation (2) under no ∇T, the voltage $U/2$ across the cathodic plate is expressed as

$$\frac{\tilde{\mu}_\mathrm{c} - \tilde{\mu}_\mathrm{v}}{e} = \frac{J}{e^2\mu}\int_{x_\mathrm{c}}^{0}\frac{\mathrm{d}x}{n(x)}\,, \tag{23}$$

where $J = ej$. Denoting by A the area of the cathode and $\gamma = e^2\mu n_+$ its conductivity, $AJ = I$ and the electrical resistance $R_\mathrm{c} = U/2I$ of the cathodic plate is given by

$$R_\mathrm{c} = \frac{1}{A\gamma}\int_{x_\mathrm{c}}^{0}\frac{n_+}{n(x)}\,\mathrm{d}x. \tag{24}$$

Should $n(x)$ stay equal to the cation density n_+ until $x = 0$, the resistance $R_\mathrm{c} = |x_\mathrm{c}|/A\gamma$ would be determined by the bulk conductivity $\gamma \approx 4\text{x}10^6\ \Omega^{-1}\mathrm{m}^{-1}$ of tungsten at $T = 1100$ K. Since $R_\mathrm{c} \approx 10^{-6}\ \Omega$ cannot account for $I \approx 7\text{x}10^{-4}$ A flowing under $U/2 = 0.05$ V in diode EB 91, there must exist a depleted region where $n(x) << n_+$ so that the integral in (24) greatly exceeds $|x_\mathrm{c}|$.

Combining Eqs. (13), (15) and (16) yields a differential equation on function $E_\mathrm{F}(x)$ alone; see appendix B. Let x_d demarcate the degenerate region $x < x_\mathrm{d}$, where $n(x) > n_\mathrm{d}$, from the depleted region $x_\mathrm{d} < x < 0$, where $n(x) < n_\mathrm{d}$. The solutions of the differential equation in the two regions should fulfil continuity conditions at x_d. There, both $E_\mathrm{F}(x)$ and the electrochemical force driving the current are continuous. Since the Poisson equation (15) demands that $\mathrm{d}E_\mathrm{c}/\mathrm{d}x$ should be continuous, so too should $\mathrm{d}E_\mathrm{F}/\mathrm{d}x$. Solving for the differential equation governing function $E_\mathrm{F}(x)$ is possible using the method of

regional approximations, which is known to give good results in problems of current injection in and out of solids [45, 46]. This is done in appendix B and the outcome of the calculation is shown in Figure 2.

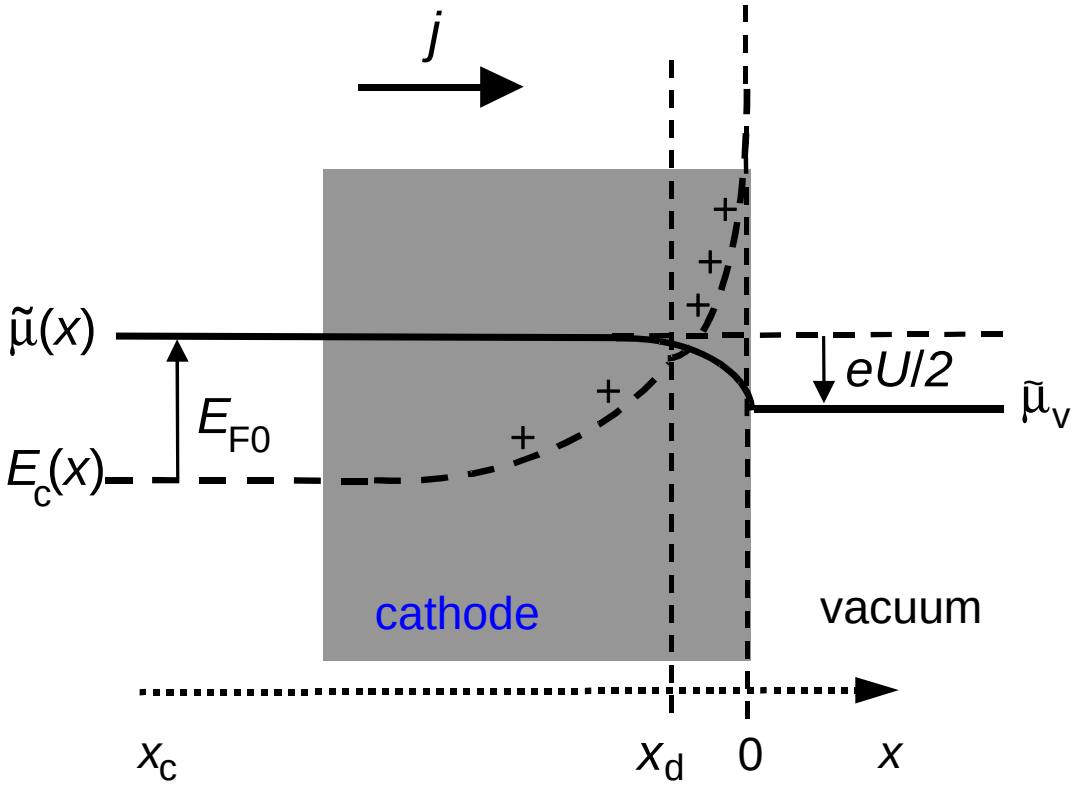

Figure 2. Energy-level diagram of the vacuum diode with electron current density j flowing rightwards, zoomed near the cathode boundary $x = 0^-$. The full line shows the electrochemical potential $\tilde{\mu}(x) = E_c(x) + E_F(x)$ starting from $\tilde{\mu}(x_c) = \tilde{\mu}_c$, and the broken line shows the bottom of the conduction band $E_c(x)$. Far before the cathode boundary, the weak negative slope $d\tilde{\mu}/dx = dE_c/dx$ is approximated to zero in the figure because $\tilde{\mu}(x_c) - \tilde{\mu}(x_d) << eU/2$. At a few Thomas-Fermi lengths before the boundary, the depletion of conduction electrons makes $E_F(x)$ drop, but the space charge bends $E_c(x)$ upwards so that the decrease of $\tilde{\mu}(x)$ is insignificant. After $E_c(x)$ overcomes $\tilde{\mu}(x)$ at $x \approx x_d$, the metal is so strongly depleted that it is effectively semiconducting.

Far before $x = 0$, the metal is neutral and the electric field $F_\infty/e = J/\gamma$ is determined by Ohm's local law. The profile of electrochemical potential $\tilde{\mu}(x) = \tilde{\mu}_c - F_\infty(x - x_c)$ is tilted accordingly, with a very weak tilt $-F_\infty$ not shown in Figure 2. The weak decrease of $\tilde{\mu}(x)$ is due to $E_c(x)$, not to $E_F(x)$. As $x \to 0$, $E_F(x)$ decreases but this decrease is almost exactly balanced by $E_c(x)$ bending upwards over the characteristic Thomas-Fermi length λ_{TF}. Beyond $x = x_d$, the electron-depleted metal becomes a semiconductor in which the decrease of $E_F(x)$ overwhelms the increase of $E_c(x)$. Eventually $\tilde{\mu}(x) = E_c(x) + E_F(x)$ goes below $E_c(x)$, and $\tilde{\mu}(x = 0)$ reaches the value $\tilde{\mu}_c - eU/2$ while it was staying nearly constant in the degenerate region, except for the weak tilt $-F_\infty$.

At the exit $x = x_d$ of the degenerate region, the electrical potential energy has risen by $\approx E_{F0} =$ 12 eV with respect to the entrance $x = x_c$. Over the interval $[x_c, x_d]$ the electric-potential difference is large (12 V) whereas the *voltage* is insignificant, just like in a *p-n* junction [27, 28]. *Electrochemically* but not electrically speaking, the interval $[x_c, x_d]$ is almost equipotential. The electrical force $-dE_c/dx = -E_{F0}/\lambda_{TF} = -6x10^{10}$ eV/m at x_d means an electric field much larger than $F_\infty/e \approx 10^{-7}$ V/m in the bulk. The electrical force at x_d is directed backwards, but electrons can reach the vacuum gap because that force is outbalanced by the "chemical" contribution to the driving force, namely $-dE_F/dx$ causing

diffusion from more to less populated places. The "chemical force" grows up more rapidly than the electrical one in the non-degenerate layer, which is why the voltage $U/2$ is essentially located in the thin deeply depleted layer at $x = 0^-$, and likewise at $x = L^+$ in the anode. In appendix B it is calculated that $|x_d| \approx 0.51\text{x}10^{-10}$ m for U lying in the range 10^{-3}-10^{-1} V.

In the next subsection we pick up prominent findings of this study of the vacuum diode in the linear regime and point out their counterparts in a solid-state ballistic resistor.

4.2 Implications of the vacuum diode study for solid-state Landauer resistors

Electric versus electrochemical potential. In the ballistic region, the functions V and n are linked through the Poisson equation and the condition $\nabla\tilde{\mu}(n, T_v) = 0$, just like in a problem of equilibrium screening. For a non-degenerate ideal gas of electrons, uniformity of $\tilde{\mu} = kT_v\ln(n\lambda_{dB}^3/g_s) + \bar{e}V(x)$ entails Boltzmann's relation $n(x) \propto \exp[-\bar{e}V(x)/kT_v]$. Thus in the ballistic region $V(x)$ is governed by a Poisson-Boltzmann equation. In equilibrium and for chemically identical reservoirs[3] the boundary conditions are symmetric about $x = L/2$. The equation has been solved elsewhere [26] and its solution is shown in Figure 3 together with $V(x)$ in the terminals. The latter are taken as metals where $V(x)$ is given by a Thomas-Fermi formula [46]. Figure 3 shows a strong discrepancy between the electric and electrochemical potential profiles in the vacuum gap. The latter profile is flat while the former shows a variation of 1.4 V between an electrode and mid-gap in EB 91 under no U. In other words, an electrical force is present while the electrochemical force and the current vanish.

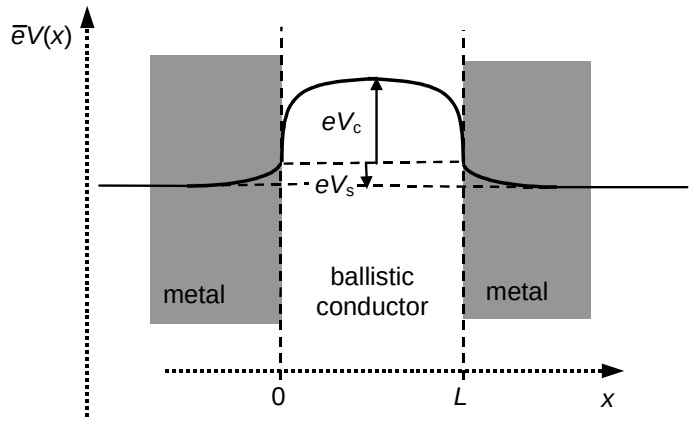

Figure 3. Electrical potential energy $\bar{e}V(x)$ in a non-degenerate ballistic conductor as a function of position x, in equilibrium ($U = 0$ and $T_c - T_a = 0$). In the metal lying at $x \le 0$, $\bar{e}V(x) = \bar{e}V(-\infty) + \bar{e}V_s\exp(x/\lambda_{TF})$ where $V_s \approx -10^{-4}$ V and $\lambda_{TF} \approx 2\text{x}10^{-10}$ m (in tungsten) have been exaggerated in the figure. In the ballistic conductor, $\bar{e}V(x) - \bar{e}V(0) = kT\ln\left(\cos^2[(x - L/2)/d']\right) + eV_c$, where $V_c = (kT/e)\ln[\cos^{-2}(L/2d')]$. In the vacuum diode EB 91 operated at $T = 1100$ K, $V_c = 1.4$ V and $d' \approx L/\pi = 1.3\text{x}10^{-4}$ m. The negative space charge in the ballistic conductor is balanced by the positive space charges in the electrodes.

In Figure 2 drawn for U in the range 10^{-3}-10^{-1} V, there is a strong discrepancy between the two potential profiles inside an electrode. The electrochemical-potential drop $eU/2$ is less than 0.05 eV while the electric-potential variation exceeds $E_{F0}/e = 12$ V in tungsten. Besides, the two potential profiles vary over distinct characteristic lengths, respectively $|x_d|$ and λ_{TF}. As a result, postulating that the two profiles track one another in a ballistic degenerate wire, as is done in figure 1 of [18] and figure 3 of [39], is unwarranted. In this connection, let us quote Landauer [6]: "Spatial variation of the self-consistent voltage distribution [...] *cannot* be done without recourse to Poisson's

[3] For chemically different reservoirs there is a Volta potential equal to the difference in the work functions reckoned in electronvolt. The Volta potential is 0.9 V in Mullard's diode EB 91 (Siemens' EAA 91).

equation, space-charge neutrality, a frequency- and wavenumber-dependent dielectric constant for the electron gas, or some other explicit way of coping with screening. [...] Papers that ignore Poisson's equation [...] cannot possibly have any bearing on the many questions related to the spatial features of the voltage drop within the system". Surprisingly, Landauer's remark is ignored in most of the works, performed until 2009, reviewed in [16]. The present paper dealing with the steady-state $V(x)$ has taken a wavenumber-*in*dependent dielectric constant for the sake of simplicity.

Kinetic-theory calculation of the Joule heating effect. The heat generation accompanying the electron flow in a solid ballistic wire was dealt with by Gurevich using a kinetic theory [21]. Heating was found to occur in the leads because of the scattering term (with phonons) in the Boltzmann kinetic equation. The agreement of kinetic theory with non-equilibrium thermodynamics is expected from their connection [13, 32]. The former, however, was worked out in [21] in the reflectionless case $\bar{t} = 1$, which precludes the very existence of an internal resistance ascribed to reflection such as invoked in [14-18]. Besides, the physical quantity of experimental relevance (voltage) does not appear in the Boltzmann kinetic equation which involves the electrical force instead of the electrochemical gradient. Accordingly no map of $\tilde{\mu}(x)$ was obtained [21, 47]. Heating was found to take place over one electronic mean free path in the ordinary conductors connected to the ballistic wire, whereas in the vacuum diode heating takes place over a length $|x_d|$ shorter than one mean free path. The difference between the wire and the vacuum diode is due to the one-dimensional guiding of electron waves within the wire. In a wire, an electron enters the ordinary conductor lying at $x > L$ (resp. $x < 0$) with no transverse motion, i.e. $v_{gy} = v_{gz} = 0$ and $v_{gx} > 0$ (resp. $v_{gx} < 0$). Therefore one free path is needed for the electron to suffer a scattering event with a phonon [48, 49]. Over a longer path the electron is transported by drift with a large scattering rate *per unit length* along x.

Role of quantum coherence. It is often stressed that a Landauer resistor is coherent. This is manifested in the transmission coefficient $t(\mathbf{p})$ of an electron of wavevector $2\pi\mathbf{p}/h$ in the interval $[0, L]$. However, any electron crossing that interval comes from one of the terminals where the microscopic dynamics is incoherent. Quantum-statistical-mechanically speaking, the equilibrium dynamics in a reservoir is described by a density matrix with vanishing coherences (off-diagonal elements) and Fermi-Dirac populations (diagonal elements). A small correction to the latter enables a departure from equilibrium; see Eq. (6). The ballistic region $[0, L]$, where electron motion proceeds in a wave-mechanistic fashion with the electron wave function governed by Schrödinger's equation involving the definite potential energy $\bar{e}V$, cannot *create* coherences. An electron wave can interfere only with its own transmitted and reflected partial waves in the coherent region. There is no definite phase relationship between partial waves from *two* electrons, so that they propagate without interfering with one another, just like two beams of natural light. This is so in a vacuum diode [50] and a solid ballistic wire [51] as well. The fact that the overall coefficient $\bar{t}$ factoring the force-driven current $I \propto U$ is given by wave mechanics although the phases of two electron waves are uncorrelated with one another is also met in force-free ($U = 0$) transport [52].

The overall transmission coefficient $\bar{t}$ is obtained from thermally averaging the probability current density of the electron waves. In the vacuum gap of a diode,

$$\bar{t} = \frac{\iiint_{v_{gx}>0} t(\mathbf{p})\, v_{gx}(\mathbf{p}) \exp[-E_k(\mathbf{p})/kT_v]\, d^3\mathbf{p}}{\iiint_{v_{gx}>0} v_{gx}(\mathbf{p}) \exp[-E_k(\mathbf{p})/kT_v]\, d^3\mathbf{p}}, \qquad (25)$$

where $\mathbf{v}_g(\mathbf{p}) = \mathbf{p}/m_0$ is the group velocity in vacuum. In a solid ballistic conductor, $\mathbf{v}_g(\mathbf{p})$ is $\partial E_k/\partial \mathbf{p}$ and Boltzmann's $\exp[-E_k(\mathbf{p})/kT_v]$ is replaced by $f(1 - f)$ so as to account for Pauli exclusion, and f is the Fermi-Dirac occupancy. Often $f(1 - f)$ is written $kT(-\partial f/\partial E)$ [2]. As $t(\mathbf{p})$ involves not only the potential profile in the range $[0, L]$ but also the periodic potentials in the contacts, it is difficult to assess theoretically. The literature [22, 23] shows that the experimental determination of $\bar{t}$ is not accurate either.

5. Conclusions

Section 1 asked the question "Where is the resistance?" in a ballistic resistor, and the issue was investigated from a thermodynamic standpoint, i.e. "resistance is isothermal dissipation". That standpoint encompasses the degenerate electron gas present at a GaAs/AlGaAs heterojunction and the non-degenerate gas of electrons in a vacuum. We used the fact that the thermodynamic variables $\tilde{\mu}$ and T are well-defined in the reservoirs serving as terminals, which impose a Fermi-Dirac occupation function at the boundaries of the ballistic region. We used the Vlasov kinetic equation to show that the occupation of the electron states is a function F of the total energy E with no position dependence in the ballistic region. Since the Fermi-Dirac shape of function F is imposed by the terminals through the boundary conditions, there exist well-defined variables $\tilde{\mu}$ and T inside the ballistic region; and they are uniform because of $F(E)$ being independent of position. In the presence of an imbalance $\tilde{\mu}_c - \tilde{\mu}_a$ or $T_c - T_a$, the ballistic region acts as an electrical and thermal short circuit between its boundaries. Inside that region, electron and entropy currents flow under no driving force, in a way reminiscent of Newton's First Law of motion in mechanics; and the thermodynamics of irreversible processes holds in the border-line case of a reversible process in which dissipation vanishes exactly. The dissipation of the whole structure, due to either $\tilde{\mu}_c - \tilde{\mu}_a$ or $T_c - T_a$, or both, arises in the terminals; and there is no internal resistance associated with wave-mechanical reflection.

The predicted uniformity of $\tilde{\mu}(x)$ is supported by a four-point probe measurement of resistance in a 6-μm-long solid ballistic wire. The predicted uniformity of $T(x)$ is observed in a vacuum diode where $T_c - T_a$ is large, but there is no guarantee that the linear relations of non-equilibrium thermodynamics should hold for a large $T_c - T_a$. The prediction of a flat temperature profile for a small $T_c - T_a$, which is a consequence of non-dissipative transport in the linear regime, may be put to experimental test.

The framework used in this paper allows one to map the dissipation, which arises in thin layers located before and after the boundaries of the ballistic transport range. The analytical calculation of the isothermal dissipation in a vacuum diode has disclosed the vastly discrepant behaviours of the electric and electrochemical potentials, regarding both their values and their characteristic variation lengths. Therefore Landauer's admonition quoted in Section 4.2 remains pertinent, making a non-equilibrium screening calculation mandatory to describe the behaviour of a full resistor made up by contacting a ballistic region with two or more non-ballistic terminals. It is hoped that the present work will foster the use of non-equilibrium-thermodynamic tools in mesoscopic conductors.

Acknowledgements. I am indebted to Ionel Solomon (CNRS & Ecole Polytechnique) for discussions about the regional approximation in conduction problems, to Vladimír Lisý (Technical University of Košice, Slovakia) and the Dubna Joint Institute for Nuclear Research (Russia) for providing me with Boguslavsky's work, to Edouard Boulat and Mohamed Hebbache (Université de Paris-7) for discussions about the relevance of electrochemical potential and the description of screening, and to Charles Hirlimann (CNRS) for discussion about his work. Thanks are due to Marc Apfel and Patrick Lepert (CNRS) for their experimental assistance, and to Ali Naji and S. Nader Rasuli for giving me the opportunity to preview this work at the Institute of Physics and Mathematics of Tehran.

Appendix A. The low-voltage current-voltage relationship of a vacuum diode

In equilibrium ($U = 0$ and $T_c - T_a = 0$), the electric-current density J_0 effused by any of the two electrodes into the gap of a vacuum diode is given by a Richardson-Dushman-type formula [22, 23, 26, 53],

$$J_0 = e\left(\frac{g_s}{\lambda_{dB}^3}\right)\frac{\langle v\rangle}{4}\exp\left(-\frac{\phi'_0}{kT}\right), \tag{26}$$

where $\langle v \rangle = (8kT/\pi m_0)^{1/2}$ is the thermal average speed of an electron in vacuum. In (26), ϕ'_0 is the energy barrier height that an electron lying at the Fermi level $\tilde{\mu}$ has to cross in order to reach the opposite electrode. The height ϕ'_0 is greater than the metal work function ϕ_0 by the electrostatic barrier eV_c in the vacuum gap, where the space charge gives rise to a potential-energy profile $\bar{e}V(x)$ shown in Figure 3. The energy to overcome is highest at mid-gap $x = L/2$ where electrons lie in a typical energy range kT above the energy level $\tilde{\mu} + \phi_0 + eV_c = \tilde{\mu} + \phi'_0$.

In the presence of the disequilibria U and $T_c - T_a$, cathodic and anodic electrons face different barriers and the activation temperatures are different. To the first order in U and $T_c - T_a$, the imbalance between the cathodic and anodic currents entails a net current density

$$J = J_0(\phi'_0, T_c) - J_0(\phi'_0 + eU, T_a) \approx \Gamma_O\left[U + \frac{\phi'_0}{e}\left(\frac{T_c - T_a}{T_{1/2}}\right)\right], \tag{27}$$

where $T_{1/2}$ denotes $(T_c + T_a)/2$ and

$$\Gamma_O = \frac{e^2}{h}\left(\frac{g_s}{\lambda_{dB}^2}\right)\exp\left(-\frac{\phi'_0}{kT_{1/2}}\right) \tag{28}$$

is a conductance per unit area. On the right-hand side of (27), a term $2kT_{1/2}$ originating in the pre-exponential factor in formula (26) has been neglected in front of ϕ'_0 because $\phi'_0 > \phi_0$ and formula (26) already assumes $\phi_0 >> kT$. The current-voltage relationship (27) is linear with an offset linear in $T_c - T_a$. The offset reflects the larger effusion from the hot electrode, similar to the differential effusion occurring between two uncharged gases held at different temperatures [54]. In (28), the factor g_s/λ_{dB}^2 is the areal density of quantum (spin ⊗ orbital) states in position space, given the thermal (Boltzmann) occupation of momentum space. The physical meaning of expression (28) is that the two electrodes are connected to one another by parallel conductance channels of cross section λ_{dB}^2 and conductance $g_s e^2/h$ each, lying at the energy level $\tilde{\mu}_v + \phi'_0$ and populated accordingly. This is just Landauer's formula in non-degenerate statistics and in the quasi-continuous limit of a large number of transverse eigenstates or conduction channels, namely $A/\lambda_{dB}^2 >> 1$.

By solving the Poisson-Boltzmann equation in vacuum [26], it has been calculated that

$$\Gamma_O = \pi^{3/2}\frac{\varepsilon_0}{L^2}\left(\frac{2kT_{1/2}}{m_0}\right)^{1/2}. \tag{29}$$

Actually Γ_O should be multiplied by the wave-mechanical transmission coefficient $\bar{t}$ of electrons crossing the metal-vacuum-metal structure; $\bar{t}$ is given by expression (25) but is hard to assess both theoretically and experimentally [22, 23].

Our theory of non-dissipative transport predicts a uniform $T(x)$ in the vacuum gap under small U and small $T_c - T_a$; see Section 3. Commercial diodes are operated under a large $T_c - T_a$. In EB 91, $T_c \approx 1100$ K for a heater voltage 6.3 V, and $T_a = 300$ K as the anode is not heated. Experimental evidence shows a well-defined electron-gas temperature when U is small [55, 56]. There is no report of a temperature gradient in vacuum although $T_c - T_a$ is large. This supports our view that there is a unique electron temperature T_v in vacuum. We are not, however, in the conditions where a linear analysis is expected to hold. The large $T_c - T_a = 800$ K exceeding the average temperature $T_{1/2} = 700$ K entails a non-linearity known as *rectification*: there is a significant slope dI/dU at $U > 0$ whereas $dI/dU \approx 0$ at $U < 0$ ([4]). Because of those different slopes, the agreement between expression (29) and experiment reported in [26] is only half-satisfactory. Accordingly the prediction of an offset $I(U = 0)$ varying linearly in $T_c - T_a$ is not observed in figure 4 of [55]. In order to sharpen the comparison between theory and experiment, we remark that expression (29) predicts a soft dependence $\Gamma_O \propto T_v^{1/2}$ on the electron-gas temperature (we let $T_{1/2} \approx T_v$ since expression (29) is derived under the assumption of a small $T_c - T_a$). From (25) the temperature dependence of $\bar{t}$ is also expected to be soft; indeed Fowler calculated $\bar{t} \propto T_v^{1/2}$ for a free-electron dispersion relation in the metal and ignoring reflection at the anode [53]. Thus we predict a soft dependence of the slope $dI/dU = \bar{t}A\Gamma_O$ on the electron-gas temperature in the range of small positive voltages, in stark contrast with the Arrhenius dependence observed at negative voltages [55].

[4] The fact that $I(-U)$ should be equal to $I(U)$ for a vanishing $T_c - T_a$ had been noted by Boguslavsky who calculated $I(-U)/I(U)$ in the high-voltage regime and in the cylindrical, instead of planar, geometry [25].

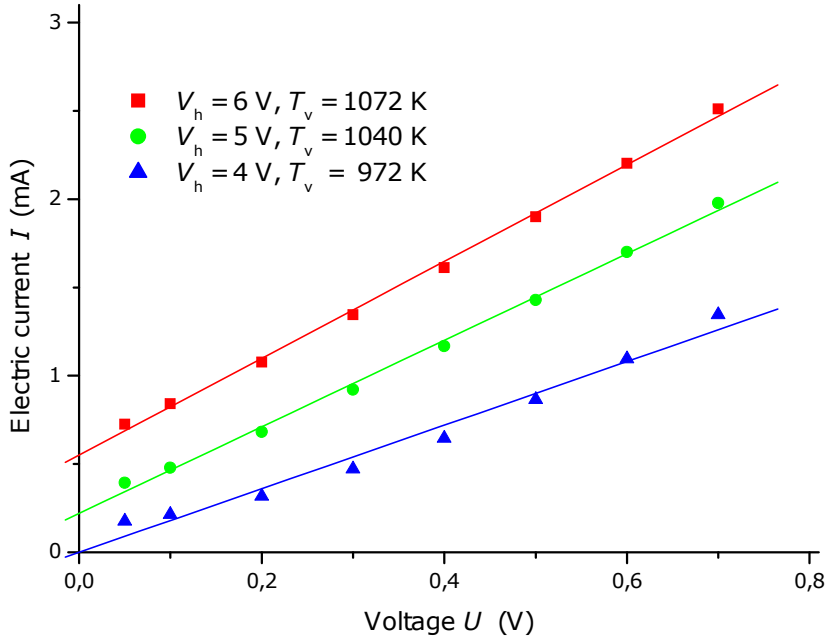

Figure 4. Experimental plot of the current (I)-voltage (U) relationship of diode EB 91 in the low-voltage range U = 0.05-0.7 V, and linear fit to the data points, with temperature T_v of the electron gas as a parameter. The correspondence between T_v and heater voltage V_h is obtained from a second-order polynomial fit to Table I of [55].

In our measurements, reported in Figure 4, the electron-gas temperature is varied between 1072 and 972 K by varying the heater voltage. It is observed that I is a fairly linear function of U in the range 0.05-0.7 V. Linear fits to the data provide the differential resistances dU/dI = 365 Ω at 1072 K, 408 Ω at 1040 K and 556 Ω at 972 K. Thus the dependence of dI/dU on the electron-gas temperature is soft, consistent with our theoretical expectation. The value of $\bar{t}$ such that $\bar{t}A\Gamma_O$ equates the experimental dI/dU is computed to be 0.37 at 1072 K, 0.34 at 1040 K and 0.26 at 972 K ([5]). Thus the dependence of the computed $\bar{t}$ on the electron temperature is soft. Not surprisingly, it differs from Fowler's calculation $\bar{t} \propto T_v^{1/2}$; but the decrease of $\bar{t}$ with T_v is expected from the fact that $t(\mathbf{p})$ vanishes for $E_k(\mathbf{p}) \to 0$ [23, 53].

Appendix B. Non-equilibrium electrochemical-potential profile in the electrodes

At $x < x_d$ where $n(x) > n_d$, the differential equation obeyed by $y(x) = 1 - E_F(x)/E_{F0}$ is

$$\frac{d^2y}{d\xi^2} - \frac{\eta}{(1-y)^2}\left(\frac{dy}{d\xi}\right) + y = 0, \tag{30}$$

where $\xi = x/\lambda_{TF}$ is a scaled position variable, $\lambda_{TF} = (\varepsilon E_{F0}/e^2 n_+)^{1/2}$ and

$$\eta = j\left(\frac{\varepsilon}{\gamma}\right)\frac{1}{\lambda_{TF} n_+}. \tag{31}$$

In equilibrium, $\eta = 0$ and equation (30) is the Thomas-Fermi equation whose solution is $y(\xi) \propto \exp(\xi)$ at $\xi < 0$. In (31), $\varepsilon/\gamma \approx 10^{-17}$ s is the dielectric relaxation time, and $\eta = 2.2\text{x}10^{-18}$ is very small at J =

[5] Estimates of L = 0.41 mm and area A = 1.4 cm^2 of Mullard's EB 91 (Siemens' EAA 91) are provided by the $I(U)$ relationship and capacitance $\varepsilon_0 A/L$ = 3 pF given by the data sheet; see www.tubedata.info. A/L^2 is obtained from equating the experimental $I(U = 14\text{ V}) = 0.1$ A to the Child-Langmuir $I(U)$ of a planar diode [26]. No significantly better accuracy is expected from the theoretical $I(U)$ in a cylindrical geometry where the agreement of the three-halves-power law with experiment has never been perfect, even at a high voltage [57].

0.5 A/m^2. Consequently the non-equilibrium term in equation (30) cannot significantly affect $y(\xi)$ unless $1 - y \approx \eta^{1/2}$, i.e. carrier depletion is very strong.

But for a strong depletion the electron gas is no longer degenerate. This occurs where $n(x) < n_d$. There, $Y(x) = E_F(x)/kT$ obeys another differential equation,

$$\frac{d^2Y}{d\Xi^2} - H\,e^{-Y(\Xi)}\left(\frac{dY}{d\Xi}\right) + 1 - \frac{N_c}{n_+}e^{Y(\Xi)} = 0, \tag{32}$$

where $\Xi = x/\lambda_D$ is another scaled position variable, $\lambda_D = (\varepsilon kT/e^2 n_+)^{1/2}$ and

$$H = j\left(\frac{\varepsilon}{\gamma}\right)\frac{1}{\lambda_D N_c}. \tag{33}$$

In equilibrium, H = 0 and equation (32) is a non-linear Debye equation. At J = 0.5 A/m^2, H = 8.6x10^{-15}. The non-equilibrium contribution in (32) can become important where $Y(x) < 0$.

At the exit $x = x_d$ of the degenerate region, continuity of E_F and dE_F/dx entails

$$Y(x_{d+}) = \frac{E_{F0}}{kT}\left[1 - y(x_{d-})\right] \approx \frac{E_{F0}}{kT}\left[\frac{N_c(T)}{n_+}\right], \tag{34}$$

$$\left(\frac{dY}{dx}\right)_{x_{d+}} = -\frac{E_{F0}}{kT}\left(\frac{dy}{dx}\right)_{x_{d-}} \quad \text{or} \quad \left(\frac{dY}{d\Xi}\right)_{x_{d+}} = -\left(\frac{E_{F0}}{kT}\right)^{1/2}\left(\frac{dy}{d\xi}\right)_{x_{d-}}. \tag{35}$$

In a degenerate electron gas where $1 - y > N_c/n_+ >> \eta^{1/2}$, equation (30) can be linearized. The solution at $\xi < 0$ is then

$$y(\xi) = y(\xi_d)\exp\left[r(\xi - \xi_d)\right], \tag{36}$$

where ξ_d is arbitrary and r is the positive root of the characteristic equation $r^2 - \eta r - 1 = 0$. From (36) we obtain the electron density,

$$n(\xi) = n_+\left(1 - y(\xi_d)\exp[r(\xi - \xi_d)]\right). \tag{37}$$

From (37), integration of the Poisson equation (15) between $\xi_c = x_c/\lambda_{TF} \approx -\infty$ and ξ provides

$$\frac{dE_c}{d\xi} = -F_\infty\lambda_{TF} + \frac{E_{F0}}{r}y(\xi), \tag{38}$$

where we have accounted for the boundary condition at $x = x_c$. The asymptotic driving force F_∞ is purely electrical since the chemical contribution $-dE_F/dx = E_{F0}(dy/dx)$ is exponentially small according to (36). Integration of (38) provides

$$E_c(x) = E_c(x_c) - F_\infty(x - x_c) + \frac{E_{F0}}{r^2}y(x). \tag{39}$$

Summing up $E_F(x)$ and $E_c(x)$ yields the electrochemical potential,

$$\tilde{\mu}(x) = \tilde{\mu}_c - F_\infty(x - x_c) - \frac{\eta E_{F0}}{r}y(x), \tag{40}$$

where we have accounted for the boundary condition $E_c(x_c) + E_{F0} = \tilde{\mu}_c$ at $x = x_c$.

At the anode, equation (30) holds with the scaled position variable $\xi' = (x' - L)/\lambda_{TF} \geq 0$. There, the solution of the linearized equation (30) is

$$y(\xi') \propto \exp(r'\xi'), \tag{41}$$

where r' is the negative root of the characteristic equation $r^2 - \eta r - 1 = 0$. Repeating the previous steps, we arrive at

$$\tilde{\mu}(\xi') = \tilde{\mu}_a - F_\infty\lambda_{TF}(\xi' - \xi'_a) - \frac{\eta E_{F0}}{r'}y(\xi'), \tag{42}$$

where ξ'_a is the scaled thickness of the anodic plate.

In (40), $F_\infty|x_c|$ is the potential-energy drop, due to the bulk electric field, over the cathodic plate. At J = 0.5 A/m^2 caused by U = 0.1 V, we compute $F_\infty = J/e\mu n_+ \approx 10^{-7}$ eV/m for an electrical conductivity $e^2\mu n_+ = 4\text{x}10^6\ \Omega^{-1}\text{m}^{-1}$. A thickness $|x_c| = 5\text{x}10^{-4}$ m of the plate entails a potential-energy drop $F_\infty|x_c| = 6\text{x}10^{-11}$ eV. As expected from Section 4.1, this is much less than $\tilde{\mu}_c - \tilde{\mu}_v = eU/2 = 5\text{x}10^{-2}$ eV.

From (40) it is seen that, besides the linear decrease of $\tilde{\mu}(x)$ due to the bulk electric field, there is a boundary effect due to lack of neutrality as $x \to 0^-$. The function $\tilde{\mu}(x)$ bends downwards as x increases. Likewise, in the anode the function $\tilde{\mu}(\xi')$ bends upwards since $y(\xi')/r' < 0$. This behaviour is

shown in Figure 1. But because $\eta << 1$, the decrease of $\tilde{\mu}(x)$ due to $y(\xi)$ is very slight compared to that of $E_F(x)$. The latter decrease is compensated for almost exactly by the increase of $E_c(x)$ due to $y(x)$. As $y(x)$ is less than unity and $r \approx 1 + \eta/2$, $\eta E_{F0} y(x)/r$ is less than $\eta E_{F0} \approx 3\text{x}10^{-17}$ eV. This cannot account for $\tilde{\mu}_c - \tilde{\mu}_v = 5\text{x}10^{-2}$ eV. Once $y(\xi)$ has reached the non-degeneracy limit $1 - N_c/n_+$ at $\xi = \xi_d < 0$, expression (36) reliant upon degenerate statistics becomes irrelevant.

But in the non-degenerate region $x > x_d = \lambda_{TF}\xi_d = \lambda_D \Xi_d$, the scaled Fermi energy $E_F(x)/kT = Y(\Xi)$ is governed by equation (32), namely

$$\frac{d^2Y}{d\Xi^2} - H e^{-Y(\Xi)}\left(\frac{dY}{d\Xi}\right) + 1 - \frac{N_c}{n_+} e^{Y(\Xi)} = 0. \tag{43}$$

The fourth term is always negligible as $Y(\Xi) \le Y(\Xi_d) = E_{F0}N_c/kTn_+ \approx 0.1$ and $N_c/n_+ << 1$. The second term may be neglected in front of unity if $Y(\Xi) > \ln[H(-dY/d\Xi)]$. This allows us to implement the method of regional approximations appropriate to problems of current injection in and out of solids [45, 46]. Not far beyond Ξ_d the regional approximation of equation (43) is

$$\frac{d^2Y}{d\Xi^2} + 1 \approx 0, \tag{44}$$

with the boundary conditions (34) and (35) at $\Xi = \Xi_d$, namely

$$Y(\Xi_d) = \frac{N_c}{n_+}{\Xi_0}^2 \quad \text{and} \quad \left(\frac{dY}{d\Xi}\right)_d = -\Xi_0, \tag{45}$$

where Ξ_0 denotes $(E_{F0}/kT)^{1/2}$. The solution of equations (44)-(45) is

$$Y(\Xi) = \frac{N_c}{n_+}{\Xi_0}^2 - \Xi_0(\Xi - \Xi_d) - \frac{1}{2}(\Xi - \Xi_d)^2. \tag{46}$$

The solution is valid till $\Xi = 0$ unless $Y(\Xi)$ decreases below $\ln[H(-dY/d\Xi)]$ at some cross-over scaled position $\Xi_{co} < 0$. As $-dY/d\Xi = \Xi_0 - \Xi_d + \Xi$ varies between Ξ_0 and $\Xi_0 - \Xi_d$, we may take $\ln[H(-dY/d\Xi)] \approx \ln(H\Xi_0)$. The cross-over Ξ_{co} is given by

$$\Xi_{co} - \Xi_d = \Xi_0\left(\left[1 + \frac{2N_c}{n_+} - \frac{2\ln(H\Xi_0)}{{\Xi_0}^2}\right]^{1/2} - 1\right). \tag{47}$$

There is no cross-over, i.e. $\Xi_{co} = 0$, if the voltage U is so low that $Y(\Xi = 0) = (N_c/n_+){\Xi_0}^2 + \Xi_0\Xi_d + {\Xi_d}^2/2$ given by (46) stays above $\ln(H\Xi_0)$. We shall denote by U_{co} the corresponding upper value of U.

At $\Xi > \Xi_{co}$, the regional approximation of equation (43) is obtained by neglecting the third and fourth terms. Integration of the approximate differential equation between Ξ_{co} and Ξ subject to the continuity conditions at Ξ_{co} yields

$$\frac{dY}{d\Xi} + H e^{-Y(\Xi)} = -(\Xi_0 - \Xi_d + \Xi_{co}) + H e^{-Y(\Xi_{co})} = -{\Xi_1}^{-1}, \tag{48}$$

where ${\Xi_1}^{-1}$ denotes $\Xi_0\left[1 + \frac{2N_c}{n_+} - \frac{2\ln(H\Xi_0)}{{\Xi_0}^2}\right]^{1/2} - {\Xi_0}^{-1}$. The differential equation (48) may be rewritten as

$$\frac{d[e^{Y(\Xi)}]}{d\Xi} + \frac{e^{Y(\Xi)}}{\Xi_1} = -H. \tag{49}$$

Integration of equation (49) between Ξ_{co} and Ξ subject to $Y(\Xi_{co}) = \ln(H\Xi_0)$ yields

$$\exp[Y(\Xi)] = H(\Xi_0 + \Xi_1)\exp\left(\frac{\Xi_{co} - \Xi}{\Xi_1}\right) - H\Xi_1. \tag{50}$$

Over the range $[\Xi_d, 0]$, we have to sum up two regional contributions,

$$\frac{N_c}{\lambda_D}\int_{x_d}^{0}\frac{dx}{n(x)} = \int_{\Xi_d}^{\Xi_{co}}\exp\left[-\frac{N_c}{n_+}{\Xi_0}^2 + \Xi_0(\Xi - \Xi_d) + \frac{1}{2}(\Xi - \Xi_d)^2\right]d\Xi + \int_{\Xi_{co}}^{0}\frac{d\Xi}{H(\Xi_0 + \Xi_1)\exp[(\Xi_{co} - \Xi)/\Xi_1] - H\Xi_1}. \tag{51}$$

From relation (23) the left-hand side of (51) is equal to $(N_c/\lambda_D)(eU\mu/2j) = eU/2kT\mathrm{H}$ (the contribution from the interval $[x_c, x_d]$ is negligible). On the right-hand side, the second integral is $-\mathrm{H}^{-1}\ln\{1 - (\Xi_1/\Xi_0)[\exp(-\Xi_{co}/\Xi_1) - 1]\}$. The first integral can be estimated by means of an integration by parts,

$$\int_{X_0}^{X_0 + X_d} \exp\left(\frac{X^2}{2}\right) dX = \int_{X_0^2/2}^{(X_0 + X_d)^2/2} \frac{\exp(y)\, dy}{(2y)^{1/2}} \approx \frac{\exp\left(\frac{(X_0 + X_d)^2}{2}\right)}{X_0 + X_d} - \frac{\exp\left(\frac{X_0^2}{2}\right)}{X_0}, \qquad (52)$$

and only the first contribution to the right-hand side of (52) matters if $(X_0 + X_d)^2 - X_0^2 >> 1$. Thus, (51) becomes

$$\frac{eU}{2kT} = \frac{1}{\Xi_0^2}\left[1 + \frac{2N_c}{n_+} - \frac{2\ln(\mathrm{H}\Xi_0)}{\Xi_0^2}\right]^{-1/2} - \ln\left(1 - \frac{\Xi_1}{\Xi_0}\left[\exp\left(-\frac{\Xi_{co}}{\Xi_1}\right) - 1\right]\right). \qquad (53)$$

Since the first two terms of (53) are less than unity, the logarithm may be expanded to the first order, whence

$$\exp\left(-\frac{\Xi_{co}}{\Xi_1}\right) \approx 1 + \frac{\Xi_0}{\Xi_1}\left(\frac{eU}{2kT} - \frac{1}{\Xi_0^2}\left[1 + \frac{2N_c}{n_+} - \frac{2\ln(\mathrm{H}\Xi_0)}{\Xi_0^2}\right]^{-1/2}\right). \qquad (54)$$

Replacing Ξ_1 on the right-hand side with its definition yields Ξ_{co} as a function of U through

$$\exp\left(-\frac{\Xi_{co}}{\Xi_1}\right) = \left(\Xi_0^2\left[1 + \frac{2N_c}{n_+} - \frac{2\ln(\mathrm{H}\Xi_0)}{\Xi_0^2}\right]^{1/2} - 1\right)\frac{eU}{2kT} + \frac{1}{\Xi_0^2}\left[1 + \frac{2N_c}{n_+} - \frac{2\ln(\mathrm{H}\Xi_0)}{\Xi_0^2}\right]^{-1/2}, \qquad (55)$$

keeping in mind that U is also present in $\mathrm{H} \propto U$. Once Ξ_{co} is known, the scaled depletion length $|\Xi_d|$ is obtained from (47). At $U = 0.1$ V and $J = 0.5$ A/m^2, it is computed that $|\Xi_{co}| = 0.32$ and $|\Xi_d| = 2.81$.

Relation (53) holds only if $U > U_{co}$. The voltage U_{co} above which equation (43) has been solved piecewise (regionally) over the interval $[\Xi_d, 0]$ is given by

$$\frac{eU_{co}}{2kT} = \frac{1}{\Xi_0^2}\left[1 + \frac{2N_c}{n_+} - \frac{2\ln(\mathrm{H}\Xi_0)}{\Xi_0^2}\right]^{-1/2}. \qquad (56)$$

One can obtain U_{co} iteratively, starting from the value $\mathrm{H} = 8.6\text{x}10^{-15}$ at $U = 0.1$ V and $J = 0.5$ A/m^2, to compute a first estimate of U_{co}. Then, an improved value of H is $1.2\text{x}10^{-16}$, etc. Eventually one obtains $U_{co} = 1.3\text{x}10^{-3}$ V. From (47) where $\Xi_{co} = 0$, the associated $|\Xi_d| = 2.80$ is hardly less than its value at $U = 10^{-1}$ V. We shall not investigate the range $U < U_{co}$.

References

[1] R. Landauer, Can a length of perfect conductor have a resistance?, *Phys. Lett.* **85A** (1981) 91-93.

[2] J. Sinkonnen, S. Eränen and T. Stubb, Linear conductance of short semiconductor structures, *Phys. Rev. B* **30** (1984) 4813-4815 .

[3] B. J. van Wees, H. van Houten, C. W. J. Beenakker, J. G. Williamson, L. P. Kouwenhoven, D. van der Marel et al., Quantized conductance of point contacts in a two-dimensional electron gas, *Phys. Rev. Lett.* **60** (1988) 848-850.

[4] D. A. Wharam, T. J. Thornton, R. Newbury, M. Pepper, H. Ahmed, J. E. F. Frost et al., One-dimensional transport and the quantisation of the ballistic resistance, *J. Phys. C* **21** (1988) L209-L214.

[5] H. van Houten, C. W. J. Beenakker and B. J. van Wees, Quantum point contacts, in: *Nanostructured Systems*, Semiconductors and Semimetals **35**, Academic, Boston (1992).

[6] R. Landauer, Conductance determined by transmission: probes and quantised constriction resistance, *J. Phys.: Condens. Matter* **1** (1989) 8099-8110.

[7] J. K. Gimzewski and R. Möller, Transition from the tunneling regime to point contact studied using scanning tunneling microscopy, *Phys. Rev. B* **36** (1987) 1284-1287.

[8] C. Z. Li, A. Bogazi, W. Huang and N. J. Tao, Fabrication of stable metallic nanowires with quantized conductance, *Nanotechnology* **10** (1999) 221-223.

[9] R. Landauer, Nonlinearity: Historical and Technological View, in: *Nonlinearity in Condensed Matter*, Springer Series in Solid-State Sciences **69**, Springer, Berlin (1987), 2-22.

[10] R. Landauer, Conductance is transmission, in: *Nanowires*, Kluwer, Dordrecht (1997) 1-7.
[11] Y. Imry and R. Landauer, Conductance viewed as transmission, *Rev. Mod. Phys.* **71** (1999) S306-S312.
[12] C. A. Domenicali, Irreversible thermodynamics of thermoelectricity, *Rev. Mod. Phys.* **26** (1954) 237-275.
[13] A. C. Smith, J. F. Janak and R. B. Adler, *Electronic Conduction in Solids*, McGraw-Hill, New York, 1967.
[14] S. Datta, *Electronic Transport in Mesoscopic Systems*, p. 65, Cambridge University Press, Cambridge, 1995.
[15] Y. Imry, *Introduction to Mesoscopic Physics*, 2nd ed., pp. 87-97, Oxford University Press, Oxford, 2002.
[16] D. K. Ferry, S. Goodnick and J. P. Bird, *Transport in Nanostructures*, 2nd ed., Cambridge University Press, Cambridge, 2009.
[17] B. I. Halperin and D. J. Bergman, Heterogeneity and disorder : Contributions of Rolf Landauer, *Physica B* **405** (2010) 2908-2014.
[18] G. B. Lesovik and I. A. Sadovskyy, Scattering matrix approach to the description of quantum electron transport, *Uspekhi Fiz. Nauk* **181** (2011) 1041-1096 (in Russian); *Physics-Uspekhi* **54** (2011) 1007-1059 (Engl. transl.).
[19] M. P. Das and F. Green, Landauer formula without Landauer's assumptions, *J. Phys.: Condens. Matter* **15** (2003) L687–L693.
[20] M. P. Das and F. Green, Mesoscopic transport revisited, *J. Phys.: Condens. Matter* **21** (2009) 101001.
[21] V. L. Gurevich, Heat generation by a ballistic Landauer resistor, *Pis'ma Zh. Eksp. Teor. Fiz.* **63** (1996) 61-66; *JETP Lett.* **63** (1996) 70-75; V. L. Gurevich, Heat generation by electric current in nanostructures, *Phys. Rev. B* **55** (1997) 4522-4529.
[22] C. Herring and M. H. Nichols, Thermionic emission, *Rev. Mod. Phys.* **21** (1949) 185-270
[23] W. B. Nottingham, Thermionic emission., in: *Handbuch der Physik* **XXI**, Springer, Berlin (1956), pp. 1-178.
[24] I. Langmuir, The effect of space charge and initial velocities on the potential distribution and thermionic current between parallel plane electrodes, *Phys. Rev.* **21** (1923) 419-435.
[25] S. A. Boguslavsky, The influence of space charge on the intensity of thermionic current, *Trudy Gos. eksp. el.-tekhn. Inst.* **3** (1924) 18-22 (in Russian); reprinted in S. A. Boguslavsky, *Selected Papers in Physics*, pp. 420-424, Fizmatgiz, Moscow, 1961.
[26] E. Bringuier, The electrical resistance of vacuum, *Eur. J. Phys.* **34** (2013) 931-952.
[27] W. Shockley, *Electrons and Holes in Semiconductors*, pp. 305 and 463, Van Nostrand, New York, 1950.
[28] N. W. Ashcroft and N. D. Mermin, *Solid State Physics*, pp. 257 and 592, Holt, Rinehart and Winston, New York, 1976.
[29] K. Nakashima and N. Takeyama, Steady-state thermodynamics and thermopower of metals, *J. Phys. Soc. Japan* **63** (1994) 1216-1217.
[30] E. Bringuier, Gauge-invariant approach to thermodiffusion in a liquid binary mixture, *Physica A* **390** (2011) 1861-1875.
E. Bringuier, Simple ideas about thermodiffusion in a liquid binary mixture, *C. R. Mecanique* **341** (2013) 365-371.
[31] E. Bringuier, The frictionless damping of a piston in thermodynamics, *Eur. J. Phys.* **36** (2015) 055024.
[32] H. J. Kreuzer, *Nonequilibrium Thermodynamics and its Statistical Foundations*, pp. 177-188, Clarendon Press, Oxford, 1981.
[33] E. Bringuier, Nonequilibrium statistical mechanics of drifting particles, *Phys. Rev. E* **61** (2000) 6351-6358.
[34] R. Balescu, *Equilibrium and Non-Equilibrium Statistical Mechanics*, pp. 413-421, Wiley, New York, 1975.

[35] E. H. Rhoderick, Comments on the conduction mechanism in Schottky diodes, *J. Phys. D* **5** (1972) 1920-1929.
E. H. Rhoderick and R. H. Williams, *Metal-Semiconductor Contacts*, 2nd ed., pp. 90-109, Clarendon Press, Oxford, 1988.
[36] N. Ben Abdallah, A hybrid kinetic-quantum model for stationary electron transport, *J. Stat. Phys.* **90** (1998) 627-662.
[37] L. D. Landau and E. M. Lifshitz, *Statistical Physics*, 3rd ed. Part 1, section 121, Butterworth-Heinemann, Oxford, 1980.
[38] B. K. Ridley, *Quantum Processes in Semiconductors*, 4th ed., section 12.4, Clarendon Press, Oxford, 1999.
[39] R. de Picciotto, H. L. Stormer, L. N. Pfeiffer, K. W. Baldwin and K. W. West, Four-terminal resistance of a ballistic quantum wire, *Nature* **411** (2001) 51-54.
[40] S. Yamamoto, Fundamental physics of vacuum electron sources, *Rep. Progr. Phys.* **69** (2006) 181-232.
[41] N. Morgulis, The Schottky effect for composite semi-conductor electron emitters, *Zh. Eksp. Teor. Fiz.* **16** (1946) 959-964 (in Russian); N. Morgulis, *J. Phys. USSR* **9** (1947) 67-71 (Engl. transl.).
N. D. Morgulis, Sovremenniye termoelectroniye katodiy, *Uspekhi Fiz. Nauk* **LIII** (1954) 501-543; N. D. Morgulis, Moderne Thermokathoden, *Forts. der Physik* **3** (1955) 57-95 (German transl.).
[42] D. A. Wright and J. Woods, The emission from oxide-coated cathodes in an accelerating field, *Proc. Phys. Soc. B* **65** (1952) 134-148.
[43] H. J. F. Jansen and A. J. Freeman, Total-energy full-potential linearized augmented-plane-wave method for bulk solids: Electronic and structural properties of tungsten, *Phys. Rev. B* **30** (1984) 561-569.
[44] J. S. Blakemore, *Semiconductor Statistics*, pp. 80-81, Dover, New York, 1987.
[45] M. A. Lampert and P. Mark, *Current Injection in Solids*, pp. 50, 60 and 66, Academic Press, New York, 1970.
[46] J.-N. Chazalviel, *Coulomb Screening by Mobile Charges*, p. 248, Birkhäuser, Boston, 1999.
[47] V. L. Gurevich, V. I. Kozub and M. I. Muradov, Dynamical response of nanostructures and Joule heat release, *J. Phys.: Condens. Matter* **23** (2011) 405302.
[48] B. K. Ridley, Lucky-drift mechanism for impact ionisation in semiconductors, *J. Phys. C* **16** (1983) 3373-3388.
[49] E. Bringuier, Fokker-Planck approach to nonlocal high-field transport, *Phys. Rev. B* **56** (1997) 5328-5331.
[50] N. H. Frank, Thermionic emission and space charge, *Phys. Rev.* **39** (1932) 226-236.
[51] R. Landauer, Residual resistivity dipoles, *Z. Phys. B* **21** (1975) 247-254.
[52] S. Godoy and L. S. García-Colín, Compatibility of Landauer diffusion coefficient with classical transport theory, *Physica A* **268** (1999) 65-74.
[53] R. H. Fowler, *Statistical Mechanics*, 2nd ed., Chapter 11, Cambridge University Press, London, 1936.
[54] F. Reif, *Fundamentals of Statistical and Thermal Physics*, pp. 273-280, McGraw-Hill, New York, 1965.
[55] K. Turvey, Test of validity of Maxwellian statistics for electrons thermionically emitted from an oxide cathode, *Eur. J. Phys.* **11** (1990) 51-59.
[56] O. R. Battaglia, C. Fazio, I. Guastella and R. M. Sperandeo-Mineo, An experiment on the velocity distribution of thermionic electrons, *Am. J. Phys.* **78** (2010) 1302-1308.
[57] E. L. E. Wheatcroft, The theory of the thermionic diode, *J. Inst. Elec. Eng.* **86** (1940) 473-484.